

**Ba<sub>2</sub>YCu<sub>3</sub>O<sub>7- $\delta$</sub> : Electrodynamics of Crystals with High Reflectivity**G. A. Thomas, J. Orenstein, D. H. Rapkine, M. Capizzi,<sup>(a)</sup> A. J. Millis, R. N. Bhatt, L. F. Schneemeyer, and J. V. Waszczak*AT&T Bell Laboratories, Murray Hill, New Jersey 07974*

(Received 5 May 1988)

We present results for the reflectivity,  $R$ , of two bulk crystals of Ba<sub>2</sub>YCu<sub>3</sub>O<sub>7- $\delta$</sub>  which, below the superconducting transition at  $T_c$ , show behavior consistent with perfect reflectivity up to an energy of  $(3-4)k_B T_c$ . We interpret the reproducibility and high  $R$  values (especially  $R \sim 1$  below  $T_c$ ) as indicative of intrinsic behavior in the highly conducting crystal planes probed by the light. Results above  $T_c$  show that the charge carriers have an enhanced effective mass and low scattering rate at low frequency and temperature, indicating a strong interaction with some excitation.

PACS numbers: 78.30.Er, 74.70.Vy

We have studied the absolute optical reflectivity,  $R$ , as a function of frequency,  $\omega$ , and temperature,  $T$ , of a series of bulk, crystalline samples of Ba<sub>2</sub>YCu<sub>3</sub>O<sub>7- $\delta$</sub> . These crystals<sup>1</sup> have negligible misalignment of the  $c$  axis but are microtwinned in the  $(a,b)$  plane. Six samples that we studied with  $T_c \sim 90$  K showed relatively low and sample-dependent  $R$  (in the range 0.85 to 0.95 near  $\omega = 200$  cm<sup>-1</sup> in the superconducting state). We have presented only a preliminary report<sup>2</sup> on one of these samples because of this variability. We have found<sup>3</sup> two crystals of Ba<sub>2</sub>YCu<sub>3</sub>O<sub>7- $\delta$</sub>  with reduced O content and  $T_c$ 's of 50 and 70 K which show higher  $R$  than the above values. Results on these samples are presented here with emphasis on the normal-state behavior of the sample with highest  $R$ . Both samples show qualitatively similar behavior: The charge carriers in the normal state interact strongly with some excitation enhancing their effective mass by a factor  $\sim 10$  at low  $\omega$  and  $T$ . As  $\omega$  and  $T$  are increased, the scattering rate increases drastically and the effective mass is reduced. For  $T \ll T_c$ , we find results consistent with  $R = 1$  for  $\omega$  below the energy gap,  $2\Delta$ . The central importance of this reproducibility and these high  $R$  values (especially  $R \sim 1$  below  $T_c$ ) is an indication of intrinsic behavior in the region of the crystals near the surface probed by the light.

$R$  was measured with focusing mirror optics and a rapid-scanning Michelson interferometer from 500 to 20000 cm<sup>-1</sup>, and with light-pipe optics and a stepping-mirror instrument from  $\sim 30$  to 900 cm<sup>-1</sup>. For all our experiments, light (with a spot diameter  $\leq 1.75$  mm) was incident at an angle  $\sim 10^\circ$  so that the electric field was predominantly in the basal plane. Our absolute uncertainty of 1% in  $R$  arises from the difficulties of verifying the precise optical alignment of the Au reference and sample at low  $T$ , from the sample to reference variation of the detector linearity (negligible at low  $\omega$ ), and from questions about the absolute  $R$  of our polished, solid Au reference. Relative uncertainties of about  $\frac{1}{2}\%$  apply to all the data, and arise partly from noise and partly from regular cavity oscillations at small  $\omega$  which have been eliminated from the data by averaging.

Figure 1 shows  $R$  of the sample with  $T_c = 50$  K as a function of  $\omega$  from  $\sim 30$  to 15000 cm<sup>-1</sup>, with the entire range in the inset and the low-frequency range in the main figure. We have fixed the magnitude by setting  $R = 1$  at low  $\omega$  for  $T = 20$  K. For this sample, the data as measured were 0.5% above 1, suggesting a higher  $R$  than the Au reference. (We use  $\nu$  in the figure for the frequency in cm<sup>-1</sup>.) Figure 2 shows an expanded view of the region of high  $R$  at low  $\omega$  for both samples. The lower part of the figure shows the crystal with slightly higher  $R$  in the normal state which was shown at higher  $\omega$  and  $T$  in Fig. 1. The data in the superconducting state, labeled  $S$ , were taken at  $T = 20$  K; the data in the normal state, labeled  $N$ , were taken just above  $T_c$ , with  $T_c$  determined from sharp transitions in the dc magnetization. Our estimates of the superconducting energy gap,  $2\Delta$ , are indicated by arrows in the figure placed at  $\omega$  where  $R$  deviates from unity ( $R$  set equal to 1 for low  $\omega$ ), and these points are plotted as a function of  $T_c$  in

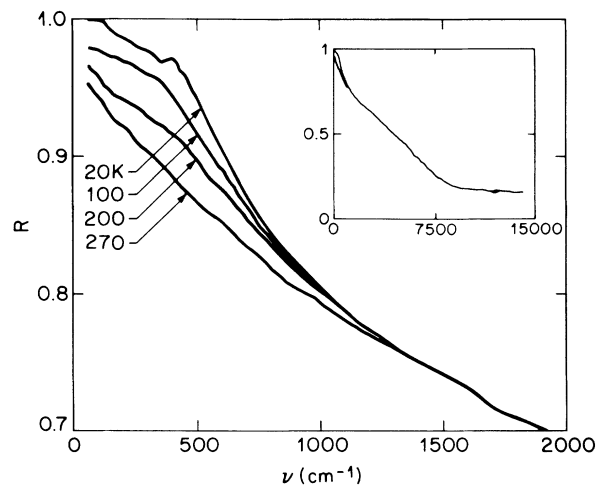


FIG. 1. Reflectivity,  $R$ , as a function of frequency,  $\nu$ , for a sample of Ba<sub>2</sub>YCu<sub>3</sub>O<sub>7- $\delta$</sub>  with  $T_c = 50$  K, at several temperatures as labeled in the main part of the figure. Inset:  $R$  over a wider range of  $\nu$  at  $T = 20$  and 270 K.

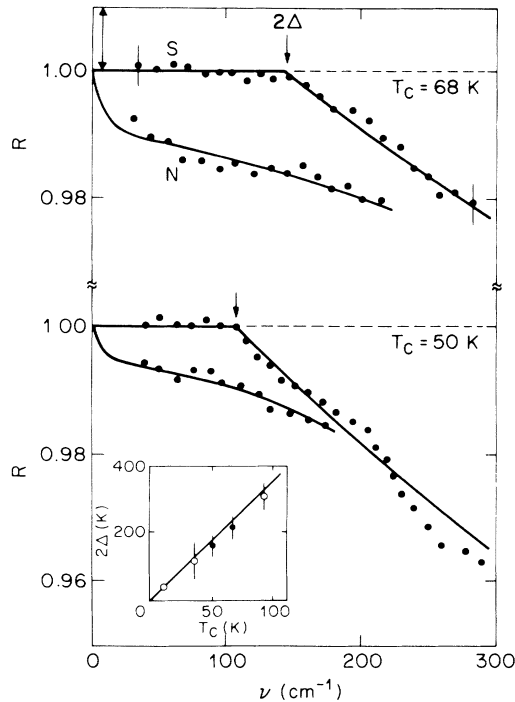


FIG. 2. Reflectivity on an expanded scale for two samples of  $\text{Ba}_2\text{YCu}_3\text{O}_{7-\delta}$  with  $T_c$  values as labeled. For each, the lower points are data just above  $T_c$  and the upper are taken at  $T=20$  K. The solid lines are guides to the eye. The arrow in the upper left indicates the absolute uncertainty in  $R$ ; the error bars on a few points indicate the relative uncertainty in  $R$  of all points. Inset: Estimates of the energy gap,  $2\Delta$ , as a function of  $T_c$  for different materials, as explained in the text, with the filled points from the data here.

the inset as filled circles. Because of our *absolute* uncertainty, we cannot rule out the possibility of  $2\Delta$  being zero; the smaller uncertainties shown in the inset arise from the *relative* error. The uncertainties in previous measurements of the gap<sup>2,4,5</sup> appear to be greater, in part because for these samples  $R < 1$  at all  $\omega$  even in the superconducting state, and the strong  $T$  dependence of  $R$  at low  $\omega$  in the normal state complicates the extraction of changes in  $R$  due to superconductivity. In the case of pressed-pellet samples with random crystal orientation, the relatively low  $R$  along the  $c$  axis and phonon absorptions substantially distort the spectrum.<sup>6-8</sup> Nonetheless, the  $2\Delta$  estimates for  $\text{Ba}_2\text{YCu}_3\text{O}_{7-\delta}$  samples<sup>6,7</sup> and  $\text{La}_{0.85}\text{Sr}_{0.15}\text{CuO}_4$  samples<sup>8</sup> are plotted in the inset as open circles. Tunneling measurements<sup>9</sup> of  $2\Delta$  in  $\text{Ba}(\text{Pb}_{1-x}\text{Bi}_x)\text{O}_3$  are also shown. The solid line is the weak-coupling BCS prediction  $2\Delta = 3.5k_B T_c$ .

We turn now to a study of the normal-state behavior of the sample with  $T_c = 50$  K. The data from the sample with  $T_c = 68$  K are similar. Figure 3 illustrates the real part of the conductivity,  $\sigma$ , obtained from the data of Fig. 1 by Kramers-Kronig (KK) transformations. To evaluate the KK integral over all  $\omega$ , we extrapolated  $R$

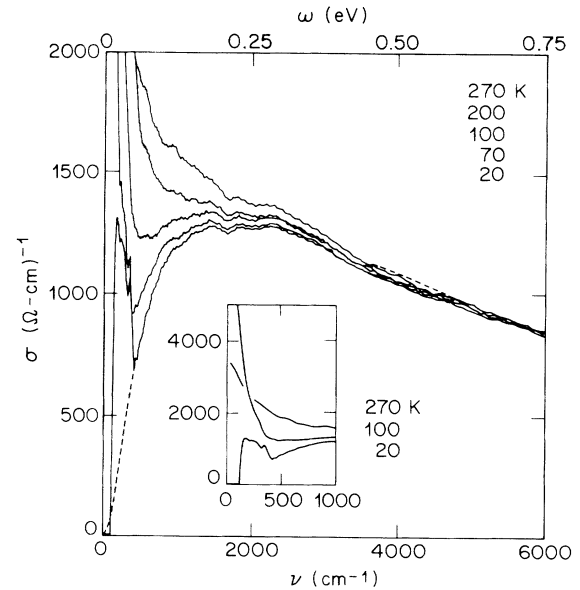


FIG. 3. Conductivity,  $\sigma$ , as a function of frequency for the same sample as in Figs. 1 and 2 (lower) obtained by KK transformation of  $R$ . The solid curves are for five different values of  $T$  as listed; the dashed curve is a damped harmonic oscillator [Eq. (1b)] fit to  $T=20$ -K data. Inset: higher  $\sigma$  values at low  $\nu$  for the three  $T$  values as listed.

to  $\omega=0$  with a Hagen-Rubens fit to the data at  $\omega \sim 30$   $\text{cm}^{-1}$ , and to  $\omega = \infty$  using a form containing  $\omega^{-4}$  as described previously.<sup>10</sup> It is clear from Fig. 3 that  $\sigma$  has a strong  $\omega$  and  $T$  dependence. Two noteworthy features are a peak, of  $T$ -dependent width and height, centered at  $\omega=0$ , and a broader peak centered at  $\omega \sim 1700$   $\text{cm}^{-1}$ . In order to provide an empirical description of the data and to estimate the total spectral weight, we fitted  $\sigma(\omega, T)$  to the sum of two conductivities: a Drude form,  $\sigma_D$ , and a damped harmonic oscillator,  $\sigma_o$ ,

$$\sigma_D(\omega, T) = (\omega_{pD}^2/4\pi)\Gamma_D/(\omega^2 + \Gamma_D^2), \quad (1a)$$

$$\sigma_o(\omega) = (\omega_{po}^2/4\pi)\omega^2\Gamma_o/[(\omega^2 - \omega_o^2)^2 + \omega^2\Gamma_o^2], \quad (1b)$$

where  $\omega_{pD} = 1$  eV (8200  $\text{cm}^{-1}$ ),  $\omega_{po} = 3$  eV (24000  $\text{cm}^{-1}$ ),  $\omega_o = 0.2$  eV (1700  $\text{cm}^{-1}$ ),  $\Gamma_o = 0.9$  eV (7500  $\text{cm}^{-1}$ ) with  $\sim 20\%$  uncertainties. The fitted scattering rates and dc conductivities at each  $T$  were as follows:  $[\Gamma_D, \sigma(0), T] = [350 \pm 50, 3200 \pm 300, 270 \text{ K}]$ ;  $[240 \pm 50, 4800 \pm 500, 200]$ ;  $[125 \pm 40, 9000 \pm 1000, 100]$ ;  $[60 \pm 40, 1500 \pm 4000, 70]$ . Within our uncertainties  $\Gamma_D(T)$  may have some  $\omega$  dependence.  $\sigma_o(\omega)$  is shown (where it is distinguishable from the data) as the dotted line in Fig. 3. A similar form of  $\sigma(\omega)$  has been shown<sup>11</sup> to describe  $R$  of textured ceramic samples of  $\text{Ba}_2\text{YCu}_3\text{O}_7$  with  $T_c \sim 90$  K. The measurements of  $R$  in these and other pressed powders<sup>10-15</sup> are distorted by anisotropy effects<sup>7</sup> but are useful for comparison.

One way of interpreting the  $\sigma(\omega, T)$  data involves associating  $\sigma_o$  with an interband transition (possibly because of a density wave as in, e.g., the spectrum<sup>16</sup> of Cr) and  $\sigma_D$  with a free carrier, Drude conductivity. A difficulty with this interpretation is that  $\omega_{pD}$  is very small [as confirmed by the fitted values of  $\Gamma_D$  and  $\sigma(0)$ ] corresponding to a carrier density of  $n \cong (0.6 \times 10^{21} \text{ cm}^{-3}) \times (m^*/m_e)$ , where  $m^*$  is the carrier effective mass and  $m_e$  is the free-electron mass. To reconcile this value with band-structure calculations, and with formal valence estimates of  $n$  (in which one assumes  $2-2\delta$  carriers per unit cell for  $\text{O}_{7-\delta}$ ) one must assume  $m^*/m_e \cong 10$ . But it is not obvious how such a mass enhancement at low  $\omega$  varies within these models.

An alternative interpretation involves the assumption that the structure in  $\sigma(\omega, T)$  arises because the carriers interact with a spectrum of other optically inactive excitations, as occurs, for example, in heavy-fermion materials<sup>17</sup> and in materials with strong electron-phonon interactions.<sup>18</sup> To make this interpretation more quantitative, it is convenient to parametrize the data in terms of a generalized Drude model, in which the complex conductivity,  $\tilde{\sigma}(\omega, T)$ , is written in terms of two real functions, an effective mass,  $m^*(\omega, T)$ , and a scattering rate,  $\Gamma(\omega, T)$ ;

$$\tilde{\sigma}(\omega, T) = (\omega_p^2/4\pi) / [-i\omega(m^*/m) + \Gamma], \quad (2)$$

where  $m$  is the bare (or optical) mass. Because  $\tilde{\sigma}$  is casual and nonvanishing in the upper half  $\omega$  plane,  $\Gamma$  and  $i\omega[(m^*/m) - 1]$  obey a KK relation. Determination of the magnitude of  $m^*$  and  $\Gamma$  requires knowledge of  $\omega_p$ , which follows from the  $f$ -sum rule,  $\int_0^\infty \sigma d\omega = \omega_p^2/8$  (where the integral is to include only the free-carrier contributions to  $\sigma$ ). We may use the fit described in Eq. (1) to parametrize  $\sigma$  (assuming both  $\sigma_D$  and  $\sigma_o$  are free-carrier contributions) obtaining  $\omega_p = 3.2 \text{ eV}$ , corresponding to a carrier density  $n = (6 \times 10^{21} \text{ cm}^{-3})(m/m_e)$ , and, assuming 2D electronic structure, to a Fermi energy  $E_F \sim 1.1 \text{ eV}$  (with 20% uncertainties). This density is in rough agreement with formal valence arguments if  $m \sim m_e$ . Using this  $\omega_p$ , our data for  $\tilde{\sigma}$ , and Eq. (2), we obtain the curves for  $m^*/m$  and  $\Gamma$  shown in Fig. 4. Note, for comparison to Eq. (1), that  $[m\Gamma(0, T)/m^*(0, T)] = \Gamma_D(T)$  while  $m^*(0, 0)/m \sim \omega_{pD}^2/\omega_{pD}^2$ .

If the variation of  $\Gamma$  and  $m^*$  is due to the interaction of carriers with a spectrum of other excitations, then  $m^*$  and  $\Gamma$  are related to the real and imaginary parts of the one-electron self-energy,  $\tilde{\Sigma} = \Sigma_1 + i\Sigma_2$ . To clarify this relationship, we have computed  $\tilde{\sigma}(\omega, T)$  and, from this,  $m^*$  and  $\Gamma$  for a model in which electrons interact with a spectrum of dispersionless oscillators, using the Migdal approximations to compute the full  $\omega$  and  $T$  dependence of the carrier self-energy, and the Kubo formula to compute  $\sigma$ . (Vertex corrections vanish for our model, and are not expected to change  $\sigma$  significantly in models

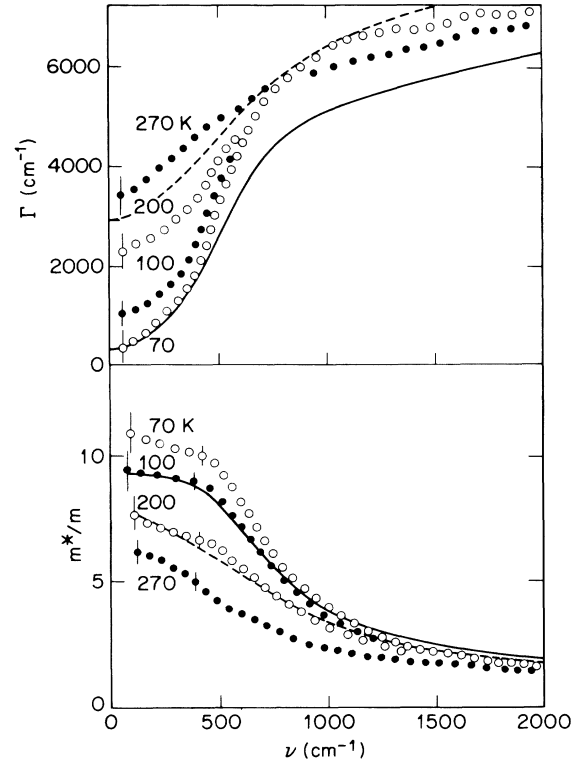


FIG. 4. Replotted data using Eq. (2) for the same sample as in Fig. 1 for four  $T$  values are listed. The upper part shows the scattering rate,  $\Gamma$ , and the lower shows the effective-mass ratio  $m^*/m$ . Curves are theoretical fits to a scattering model for  $T=100 \text{ K}$  (solid) and  $200 \text{ K}$  (dashed).

without Galilean invariance.) We have found that in both low- and high- $\omega$  limits,  $m^*/m \cong 1 - \partial\Sigma_1/\partial\omega$  and  $\Gamma = 2\Sigma_2$ . From the extrapolated  $T=0$  value of  $m^*/m = 1 + \lambda$ , we conclude that the carrier-excitation coupling constant  $\lambda \cong 9$ , indicating strong coupling. One estimate that supports a large  $\lambda$  uses the specific-heat jump at  $T_c$  in a  $\text{Ba}_2\text{YCu}_3\text{O}_7$  sample.<sup>19</sup> If we make a BCS density-of-states estimate from the jump and assume that the superconducting electrons form a 2D electron gas on the Cu-O planes, we obtain  $m^*/m \sim 12$ .

If the mid-infrared feature is due to inelastic scattering, it should shift upwards in frequency by  $2\Delta$  in the superconducting state.<sup>18</sup> However, the uncertainties described above (including the value and existence of the energy gap  $\Delta$ , normal-state thermal broadening of the mid-infrared feature, and the approximate nature of the theoretical fits) preclude at this time an analysis of the expected shift.

From the  $\omega$  at which  $m^*$  and  $\Gamma$  cross over from their low- $\omega$  to high- $\omega$  behavior, it is possible to infer the characteristic energy scale of the excitations. Specifically, a spectrum  $\phi(\omega)$  extending with equal weight from  $\omega_L = 250 \text{ cm}^{-1}$  to  $\omega_H = 550 \text{ cm}^{-1}$ , with a carrier-oscillator coupling constant  $\lambda = \int_{\omega_L}^{\omega_H} [\phi(\omega)/\omega] d\omega = 9$

reproduces  $m^*(\omega, T)$ , as shown in the curves on the lower part of Fig. 4 (dashed:  $T=200$  K, solid:  $T=100$  K). This oscillator model reproduces only the qualitative trends of  $\Gamma(\omega, T)$ ; as can be seen from the upper portion of Fig. 4, the temperature dependence is not correct at low or high  $\omega$ . The observed  $T$  independence of  $\Gamma$  at high  $\omega$  may be due to saturation of  $\Gamma$  at the Ioffe-Regel limit  $\Gamma \sim E_F$ , as  $\Gamma$  is comparable to our estimated  $E_F \sim 1.1$  eV.

In summary, we argue that the high reflectivity of the samples presented here implies that they provide a reasonable indication of intrinsic electrodynamic behavior and a possible superconducting energy gap. The detailed form of the frequency and temperature dependence of the conductivity indicates that the electrons interact strongly with some spectrum of excitations.

We would like to thank P. W. Anderson, C. Kallin, P. A. Lee, P. Littlewood, and T. Timusk for helpful comments, and B. Batlogg and L. W. Rupp, Jr., for important sample characterization.

<sup>(a)</sup>Permanent address: Istituto di Fisica G. Marconi, Rome, Italy.

<sup>1</sup>L. F. Schneemeyer, J. V. Waszczak, T. Siegrist, R. B. van Dover, L. W. Rupp, B. Batlogg, R. J. Cava, and D. W. Murphy, *Nature (London)* **328**, 601 (1987).

<sup>2</sup>G. A. Thomas, M. Capizzi, J. Orenstein, D. H. Rapkine, L. F. Schneemeyer, J. V. Waszczak, A. J. Millis, and R. N. Bhatt, *Jpn. J. Appl. Phys.* **26**, Suppl. 26-3, 2044 (1987).

<sup>3</sup>J. Orenstein, G. A. Thomas, D. H. Rapkine, A. J. Millis, L. F. Schneemeyer, and J. V. Waszczak, in *Proceedings of the International Conference on High- $T_c$  Superconductors and Materials and Mechanisms of Superconductivity*, Interlaken, Switzerland, 1988, edited by J. Müller and J. L. Olsen, *Physica C* (to be published).

<sup>4</sup>Z. Schlesinger, R. T. Collins, D. L. Kaiser, and F. Holtzberg, *Phys. Rev. Lett.* **59**, 1958, (1987).

<sup>5</sup>For a summary of early measurements of  $2\Delta$  in similar compounds, see G. A. Thomas, R. N. Bhatt, A. Millis,

R. Cava, and E. Rietman, *Jpn. J. Appl. Phys.* **26**, Suppl. 26-3, 1001 (1987).

<sup>6</sup>G. A. Thomas, H. K. Ng, A. Millis, R. N. Bhatt, R. J. Cava, E. A. Rietman, D. W. Johnson, Jr., G. P. Espinosa, and J. M. Vandenberg, *Phys. Rev. B* **36**, 846 (1987).

<sup>7</sup>J. Orenstein and D. H. Rapkine, *Phys. Rev. Lett.* **60**, 968 (1988).

<sup>8</sup>G. A. Thomas, A. Millis, R. N. Bhatt, R. J. Cava, and E. A. Rietman, *Phys. Rev. B* **36**, 736 (1987).

<sup>9</sup>B. Batlogg, J. P. Remeika, R. C. Dynes, H. Barz, A. S. Cooper, and J. P. Garno, in *Superconductivity in d- and f-Band Metals*, edited by W. Buckel and W. Weber (Kernforschungszentrum Karlsruhe GmbH, Karlsruhe, 1982); S. Tajima, S. Uchida, A. Masaki, H. Takagi, K. Kitazawa, S. Tanaka, and A. Katsue, *Phys. Rev. B* **32**, 6302 (1985).

<sup>10</sup>J. Orenstein, G. A. Thomas, D. H. Rapkine, C. G. Bethea, B. F. Levine, B. Batlogg, R. J. Cava, D. W. Johnson, Jr., and E. A. Rietman, *Phys. Rev. B* **36**, 8892 (1987); J. Orenstein, G. A. Thomas, D. H. Rapkine, C. G. Bethea, B. F. Levine, R. J. Cava, E. A. Rietman, and D. W. Johnson, Jr., *Phys. Rev. B* **36**, 729 (1987).

<sup>11</sup>D. A. Bonn, A. H. O'Reilly, J. E. Greedan, C. V. Stager, T. Timusk, K. Kamarás, and D. B. Tanner, *Phys. Rev. B* **37**, 1574 (1988).

<sup>12</sup>S. L. Herr, K. Kamarás, C. D. Porter, M. G. Doss, D. B. Tanner, D. A. Bonn, J. E. Greedan, C. V. Stager, and T. Timusk, *Phys. Rev. B* **36**, 733 (1987).

<sup>13</sup>S. Etamad, D. E. Aspnes, M. K. Kelly, R. Thompson, J.-M. Tarascon, and G. W. Hull, *Phys. Rev. B* **37**, 3396 (1988).

<sup>14</sup>K. Kamarás, C. D. Porter, M. G. Doss, S. L. Herr, D. B. Tanner, D. A. Bonn, J. E. Greedan, A. H. O'Reilly, C. V. Stager, and T. Timusk, *Phys. Rev. Lett.* **59**, 919 (1987).

<sup>15</sup>J. Orenstein, G. A. Thomas, D. H. Rapkine, C. G. Bethea, B. F. Levine, R. J. Cava, A. S. Cooper, D. W. Johnson, J. P. Remeika, and E. A. Rietman, in *Novel Superconductivity*, edited by S. A. Wolf and V. K. Kresin (Plenum, New York, 1987), p. 693.

<sup>16</sup>S. Barker, T. M. Rice, and B. I. Halperin, *Phys. Rev. Lett.* **20**, 384 (1968).

<sup>17</sup>B. C. Webb, A. J. Sievers, and T. Milalisin, *Phys. Rev. Lett.* **57**, 1951 (1987).

<sup>18</sup>For an overview, see P. B. Allen, *Phys. Rev. B* **3**, 305 (1971).

<sup>19</sup>A. Junod, A. Bezing, and J. Muller, *Physica (Amsterdam)* **152C**, 50 (1988).